

## 12. DESIGN AND DEVELOPMENT OF A MOMENTUM WHEEL WITH MAGNETIC BEARINGS

By Leo J. Veillette

NASA Goddard Space Flight Center

This paper presents the results of a contracted effort to develop a momentum wheel with radially servoed magnetic bearings. The work was performed by General Electric Company, Binghamton, New York, on NASA Contract NAS5-11440.

### COMPONENT PARTS OF MOMENTUM WHEEL

A photograph of the engineering model momentum wheel is shown in Figure 1. It consists of a mechanical assembly, suspension circuit and motor drive electronics, and control panel. The mechanical assembly includes (1) the momentum wheel, (2) magnetic bearings, (3) brushless dc spin motor, and (4) base support structure. The momentum wheel is mounted at the center of the rotor shaft and the magnetic bearings are on each end. The physical characteristics of the rotor wheel and shaft assembly are given in Table A.

A cross-sectional view of the magnetic bearing assembly is given in Figure 2. Part A in the figure is a backup ball bearing with oversized inner race diameter. A 0.1 mm (4 mils) radial gap thus exists between the rotor and the inner race of the bearing. This gap defines the normal operating range of the suspension. The axially magnetized ring magnets on the rotor shaft produce a uniform outward field in the radial position sensors (parts B) when the shaft is in the centered position. Magnetoresistors sense the change in gap flux density when the rotor shaft is radially displaced and thus provide the radial position information needed for active bearing control.

The ring magnets also produce inward flux through the 3 concentric rings in each of the axial support sections (parts C). This flux in turn produces an axial restoring force which tends to realign the rotor and stator rings whenever the shaft is axially displaced. Magnetic suspension in the axial direction is thus obtained by passive means.

The magnetic structure of the radial support section (part D) and the active control method used to achieve radial magnetic suspension are described below (Magnetic Suspension Design). The magnetic bearing characteristics are listed in Table B. The electromagnet gradient for each magnetic bearing is the same as for both bearings taken together. The nonrestoring force constant involves the destabilizing effects of both the radial and axial support sections.

Table C gives the characteristics of the brushless dc spin motor (part E).

#### MAGNETIC SUSPENSION DESIGN

Design of the axial sections of the magnetic bearings is based on the following rules:

- (1) multiple lands increase the axial stiffness proportionally as long as the gap-to-land ratio is maintained
- (2) the lands should be magnetically saturated to obtain high axial stiffness with minimum nonrestoring radial force gradient
- (3) the non-restoring force gradient increases approximately proportional to the axial force gradient (with magnetically saturated lands)

The axial suspension forces depend on the rate of change of gap reluctance with axial position.

Magnetic suspension in the radial direction is active. The radial position of the rotor shaft is controlled by two identical channels. A schematic diagram of one channel of the radial magnetic suspension is shown in Figure 3. It consists of the radial support section of the magnetic bearing, the radial position sensor, and suspension circuit electronics. The magnetic bearing radial section is constructed with 4 poles and associated coils, two along the vertical axis and two horizontal. The vertical coils,  $C_1$  and  $C_2$ , are connected in series as shown, and the winding direction is such that positive coil current produces an upward force on the rotor shaft and negative current produces a downward force.

The vertical position of the rotor shaft is sensed in the radial position sensor by using two magnetoresistors,  $M_1$  and  $M_2$ . The magnetoresistors are connected in a bridge circuit which produces a difference signal,  $e_1$ , which is proportional to the rotor shaft displacement. Signal  $e_1$  is amplified in the suspension circuit preamplifier which has an adjustable gain. The amplified output is then applied to circuits which provide system damping, compensate for rotor structural resonance, and limit saturation of the power output stage. A low frequency integrating circuit is used to give the bearing a very high static radial stiffness. The power amplifier drives the bearing electromagnet in a direction to maintain the rotor shaft suspended at the null or centered position. The suspension circuit parameters and circuit gains are readily changed to provide a wide range of suspension characteristics.

The linearized radial force characteristic of the magnetic bearing is given in Figure 4.

A detailed circuit diagram of the suspension system electronics is given in Figure 5. A Twin-tee notch filter is used to compensate for the rotor structural resonance. The sharpness of the filter notch is increased by using feedback from the low frequency integrator. The increased sharpness minimizes the effect

of the filter in reducing the suspension loop phase margin. System damping is obtained by using a combination of lead-lag and lag-lead compensation. The compensation network design and filter notch frequency are shown in the Bode diagram in Figure 6. The arrangement of lead-lags and lag-leads with respect to voltage saturation points limits the power amplifier phase lag to frequencies above the suspension loop bandwidth.

#### EXPERIMENTAL RESULTS

Two main problems which were encountered in laboratory work on the engineering model momentum wheel were (1) magnetic suspension instability due to rotor structural resonance, and (2) loss of magnetic suspension at high rotational speeds. Stable magnetic suspension was achieved by (1) stiffening the rotor wheel and shaft, (2) increasing the sharpness of the Twin-tee filter notch, and (3) use of only the inside radial position sensors. These changes served to increase the frequency separation between the rotor structural resonance and cross-over and generally to improve the phase margin of the magnetic suspension loop.

During spin-up tests, the rotor suspension successfully traversed a critical speed at 220 rad/sec., but magnetic suspension was lost at about 380 rad/sec. It is believed that dropout occurred as a result of the rotor shaft hitting the backup bearings. This in turn was caused by increased shaft wobble as the speed corresponding to the suspension servo bandwidth was approached.

Rotor balance and alignment were therefore substantially improved but these improvements resulted in only a small reduction in shaft wobble. The suspension servo bandwidth also was increased slightly as the rotor resonance increased with speed. The maximum rotor speed obtained with these changes was 500 rad/sec.

Self-lubricating Feuralon sleeve bearings were used in the initial design of the backup bearings. They caused severe chattering during even low speed dropout tests, and at high speed they were totally unsatisfactory. The Feuralon bearings were replaced by backup ball bearings and these have performed very well.

The performance characteristics of the engineering model momentum wheel have been measured and the results are listed in Table D. The maximum angular momentum obtained with the engineering model momentum wheel was 83 Nm-sec (62 ft-lb-sec) which is 83% of the design value of 100 Nm-sec (75 ft-lb-sec). The radial stiffness, under static conditions, has been measured as greater than 35,000 N/mm (200,000 lbs/in.) with the integrator included in the suspension circuit. This value compares to a stiffness of 11,000 N/mm (63,000 lbs/in.) for the steel shaft of the rotor. This means that under load, the rotor shaft displacement in the bearing magnetic field is less than 1/3 the displacement at the center of the shaft, due to bending. The radial stiffness under dynamic conditions applies, within the suspension servo bandwidth, to approximately 80 Hz.

The maximum load capability of the system is 356 N (80 lbs.) with the integrator included in the suspension circuit. It appears that the maximum design load is determined by the onset of instability caused by magnetic bearing and suspension circuit nonlinearities. With the integrator removed, however, the maximum load is limited by the backup stops. Also, the rotational losses in the magnetic bearing have been measured at speeds up to about 100 rad/sec. These losses are expected to be about  $\frac{1}{4}$  the rotational loss in a ball bearing at maximum operating speed.

#### SUMMARY AND CONCLUSIONS

An engineering model momentum wheel with radial magnetic bearings has been designed and developed and successfully operated to a speed of approximately 500 rad/sec. This speed corresponds to a maximum angular momentum of 83 Nm-sec (62 ft-lb-sec) which is 83% of the design value. The maximum momentum achieved was limited by the suspension servo bandwidth and this, in turn, was limited by the lowest structural resonance of the rotor. In any future design the maximum wheel speed, and dynamic radial stiffness as well, can be increased by using a stiffer rotor.

Also in this development, radial magnetic bearings have been shown to provide good damping and high load carrying capacity. They offer considerable flexibility in that a wide range of suspension characteristics can be obtained simply by changing some of the suspension circuit parameters.

**TABLE A**  
**PHYSICAL CHARACTERISTICS OF THE**  
**ROTOR WHEEL AND SHAFT ASSEMBLY**

<b>Rotor Assembly Diameter</b>	=	<b>40 cm (16 in.)</b>
<b>Weight</b>	=	<b>67 N (15 lbs.)</b>
<b>Shaft Length</b>	=	<b>35.6 cm (14 in.)</b>
<b>First Torsional Resonance</b>	=	<b>540 Hz</b>
<b>First Translational Resonance</b>	=	<b>702 Hz</b>

TABLE B  
MAGNETIC BEARING CHARACTERISTICS

<b>Outside Diameter</b>	=	8.9 cm (3.5 in.)
<b>Weight (per bearing)</b>	=	28 N (6.3 lbs.)
<b>Electromagnet Gradient</b>	=	75 N/amp (17 lbs/amp)
<b>Non-restoring Force Constant (per bearing)</b>	=	1136 N/mm (6.5 lbs/mil)
<b>Maximum Radial Load (per bearing)</b>	=	177 N (40 lbs.)
<b>Maximum Axial Load (per bearing)</b>	>	89 N (20 lbs.)
<b>Axial Stiffness (per bearing)</b>	=	1748 N/cm (1000 lbs/in)
<b>Position Sensor</b>		
<b>Type</b>	=	Magnetoresistor
<b>Gain</b>	=	1.38 volts/mm (35 mv/mil)

TABLE C  
BRUSHLESS DC SPIN MOTOR CHARACTERISTICS

<b>Outside Diameter</b>	=	6.98 cm (2.75 in.)
<b>Axial Length</b>	=	1.5 cm (.6 in.)
<b>Weight</b>	=	2.6 N (.6 lbs.)
<b>Type</b>	=	2 Phase
<b>Number of Poles</b>	=	6
<b>Rotor Magnet</b>	=	Alnico 6
<b>Rated Torque</b>	=	.028 mN (4 in-oz.)
<b>Peak Torque Capability</b>	=	.21 mN (30 in-oz.)

**TABLE D**  
**MOMENTUM WHEEL PERFORMANCE CHARACTERISTICS**

**Momentum**

Design Value = 100 Nm-sec  
 (75 ft-lb-sec)

Actual Max. = 83 Nm-sec  
 (62 ft-lb-sec)

**Radial Stiffness**

Static > 350,000 N/cm  
 (200,000 lbs/in.)

Dynamic = 15,750 N/cm  
 (9,000 lbs/in.)

Maximum Load Capacity = 356 N  
 (80 lbs.)

**Power**

Electronics = 7.6 watts

Bearings (full load) = 22 watts

Rotational Losses =  $3.3 \times 10^{-6}$  Nm/rad/sec.  
 (.00005 in-oz/rpm)

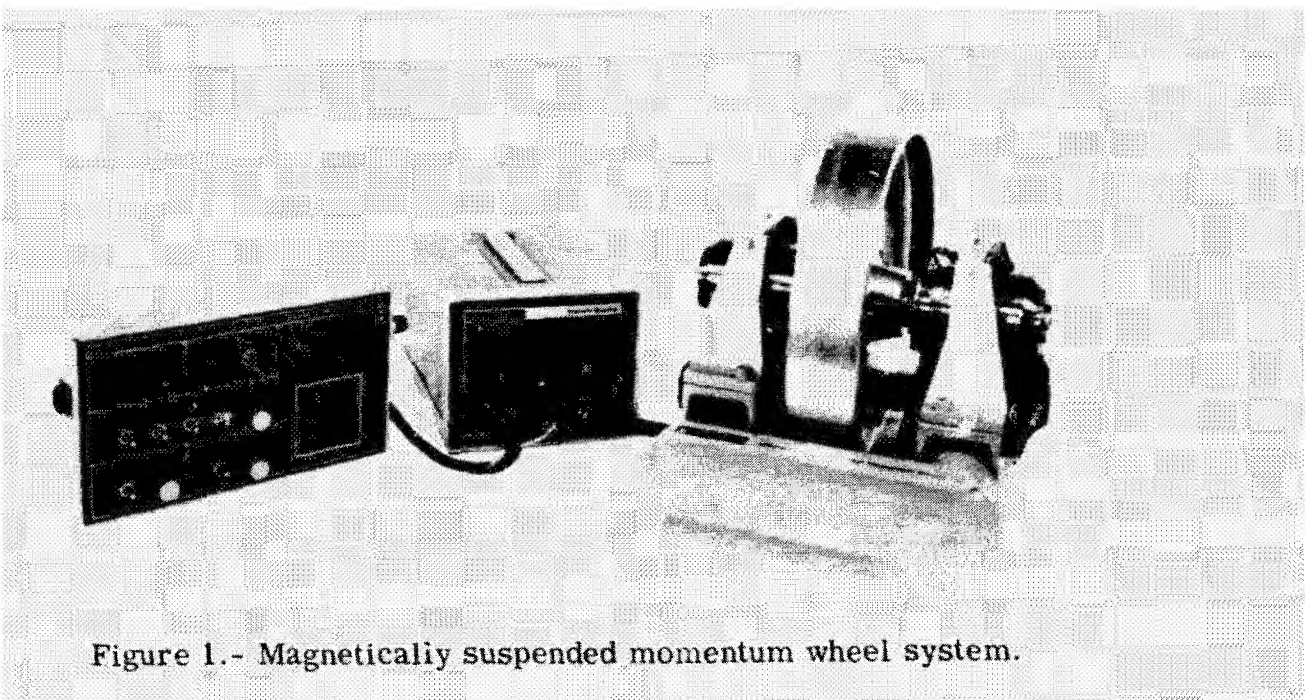


Figure 1.- Magnetically suspended momentum wheel system.

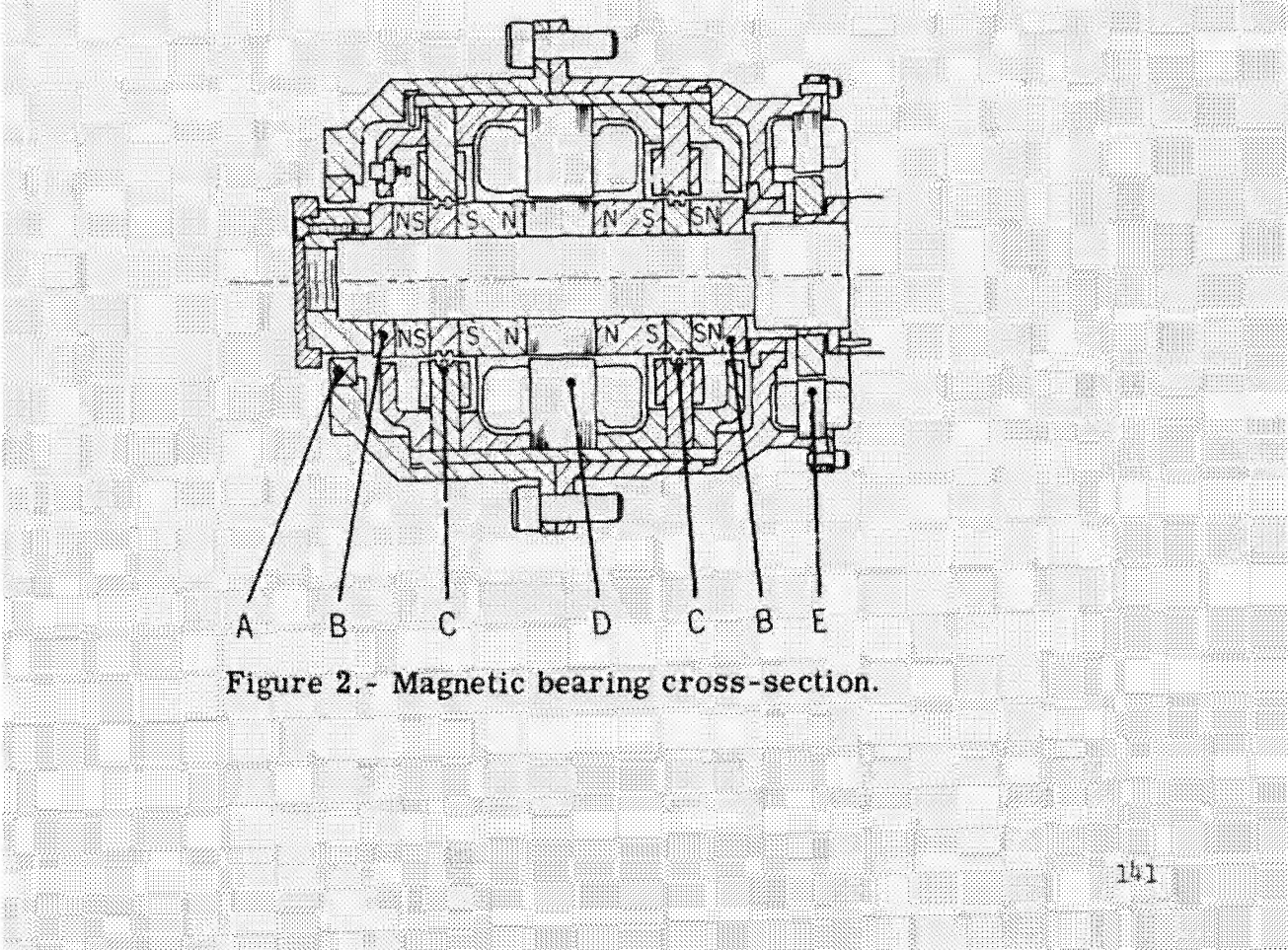


Figure 2.- Magnetic bearing cross-section.

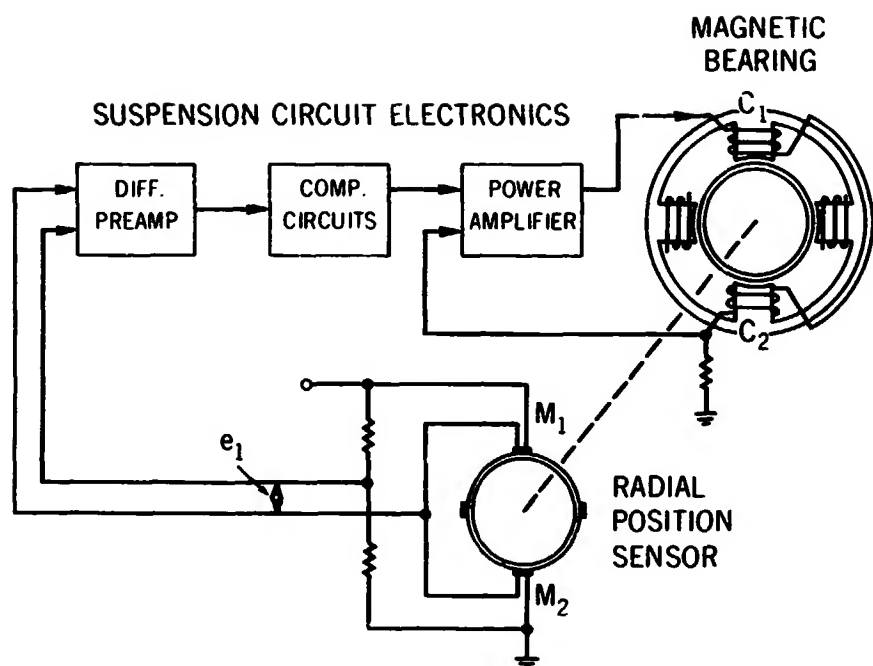


Figure 3.- Schematic diagram of magnetic suspension loop.

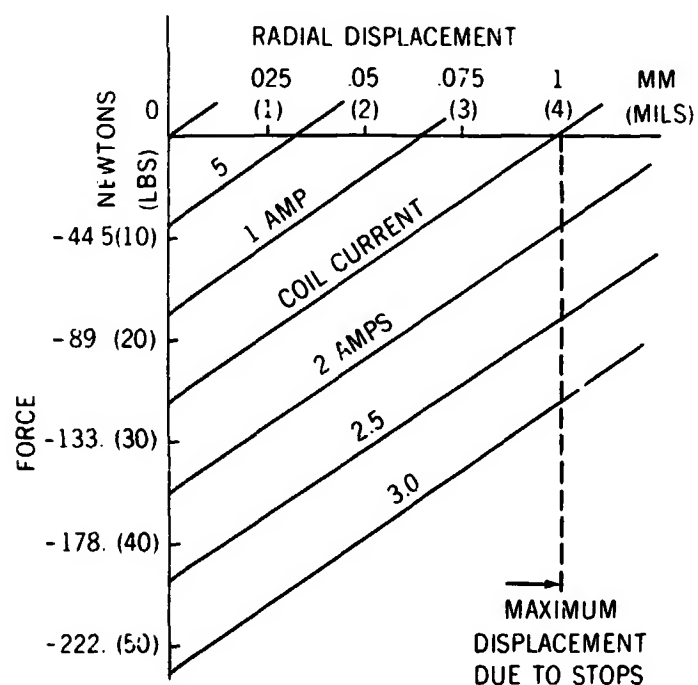


Figure 4.- Linearized magnetic bearing characteristic.

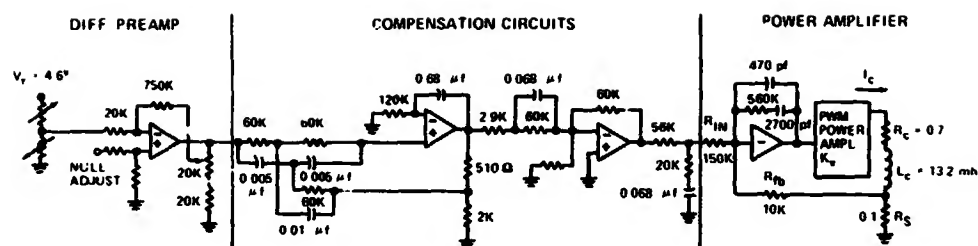


Figure 5.- Magnetic suspension electronic circuit.

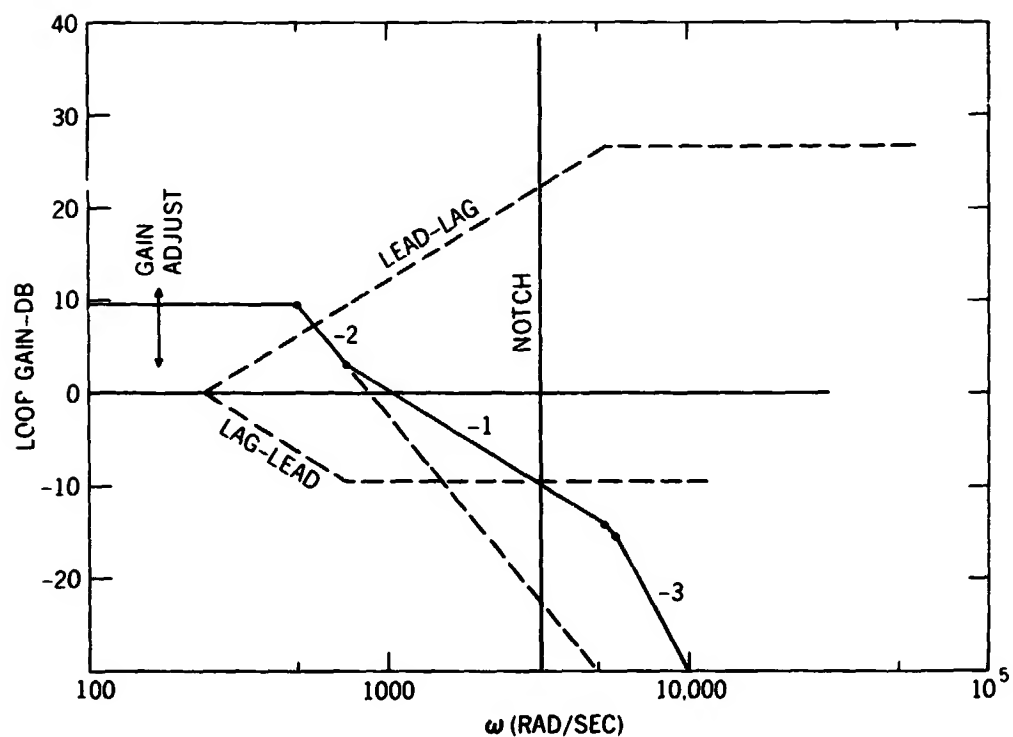


Figure 6.- Bode design of magnetic suspension loop.